IOSR Journal Of Applied Physics (IOSR-JAP)
e-ISSN: 2278-4861.Volume 14, Issue 6 Ser. I (Nov. – Dec. 2022), PP 38-44
www.Iosrjournals.Org

Preparation and Spectroscopic Studies of MWCNT incorporated PVA Nanocomposite Films for Flexible Optoelectronic Devices.

R.Venugopal[1], Rajeshwar Reddy.A[1], N. Narsimlu[1], Ch.Srinivas[1,*]
[1]*Department of Physics, University College of Engineering(Autonomous),Osmania University, Hyderabad-500007, India.*
**Email: drchsphy.ou@gmail.com*

Abstract:
MWCNT incorporated PVA nanocomposite films were prepared using the solution casting method with 0.3Wt. %, 0.6 Wt.%, and 0.9 wt.% concentration of MWCNT. The FTIR technique revealed the presence of functional groups of MWCNT. The effect of MWCNT concentration on the electrical conductivity of the PVA nanocomposites was studied. It was observed that the electrical conductivity of the nanocomposites was increased with the concentration of MWCNT. PVA with 0.9 Wt.% multi-walled carbon nanotubes loaded nanocomposite showed better electric properties. UV-Vis spectrophotometry analysis shows that adding 0.3 Wt.% MWCNT has maximum transmittance of 62.52% and minimum transmittance of 16.2 % for 0.9 Wt. % MWCNT is observed in the visible region as the concentration of MWCNT increased to 0.9 wt. % MWCNT, the PVA nanocomposites transformed from an insulator region to a semiconductor was revealed by the electrical conductivity and bandgap studies. The outcomes demonstrated that cross-linking between the nanoparticles and the polymer caused the spectroscopic properties of PVA nanocomposite films to be significantly altered with low loadings of MWCNT.

Keywords*: Polyvinyl Alcohol (PVA), Multiwall Carbon Nanotubes (MWCNT), Nanocomposite, and Spectroscopic techniques.*

Date of Submission: 07-12-2022 Date of Acceptance: 21-12-2022

I. Introduction

New materials known as polymer nanocomposites contain two or more phases, one of which is nanoscale [1]. The new material was expected to have revolutionary electrical, optical, and mechanical properties. All these characteristics are required for transparent conductive films used in light-emitting diodes, solar cells, and optoelectronic devices. The first generation of electrodes uses substantially lower peak processing temperatures than the techniques utilized for decades to create transparent electrodes on glass. At high temperatures (between 300 and 600 °C), transparent conducting oxides (TCOs), including indium tin oxide (ITO), tin oxide, and zinc oxide (ZnO), are sputtered onto the glass [2]. ITO has a low electrical resistivity ($10^{-4}\Omega$cm) and outstanding optical transparency (N90%) [3].

Since their discovery by Iijima in 1991, carbon nanotubes (CNTs) have drawn much interest because of their distinctive physical characteristics [4]. CNTs composite has been the subject of intense research materials with improved thermal, electrical, and mechanical characteristics. With several benefits, carbon nanotube (CNT) films are emerging as a possible replacement for TCOs. CNT films are excellent for roll-to-roll manufacturing because they can be treated from solution at room temperature [5]. The Young's modulus of CNTs can reach 1 TPa, and their tensile strength is close to 63 GPa [6]. Comparable in price to ITO-based films are CNT-based transparent films. For many applications, CNT-based films may also be created with sheet resistance and transmission properties that are equivalent to ITO on PET. The DC conductivity of CNT films should continue to rise as CNT materials continue to advance. Reduced reflection, more neutral hue, acid resistance, ease of laser patterning, capacity to cover uneven or curved surfaces and improved IR transmission are other benefits that CNT films have over TCOs [7]. The results of characterizations of the nanocomposite system's morphological, electrical, and mechanical properties are discussed.

II. Material And Methods

Materials:

Polyvinyl alcohol which was 95% hydrolyzed, was supplied by SD Fine Chem Ltd with a Molecular Weight range of 95,000-1,25000. Multi-wall carbon nanotubes (MWCNTs) of 20 nm diameter and length of 50μm were supplied from Ad-Nano Technologies Ltd., Bangalore, India.

PVA-MWCNT Nanocomposite film Preparation:

Different carbon nanotube loadings in free-standing PVA composite films were created. The solution casting technique was used to create PVA/MWCNT nanocomposites. A mechanical stirrer was used in a typical solution casting technique to dissolve 5 g of PVA in 80 mL of distilled water at ambient temperature. Desired Wt. % of MWCNTs were dispersed in water and added to the prepared PVA gel, and the mixture was agitated to achieve homogeneity. The uniform mixture was then poured into the dish and dried at room temperature. By adjusting the MWCNT concentration to 0.3 Wt. %, 0.6 Wt. %, and 0.9 Wt. %, multiple sets of PVA/MWCNT nanocomposite films were created.

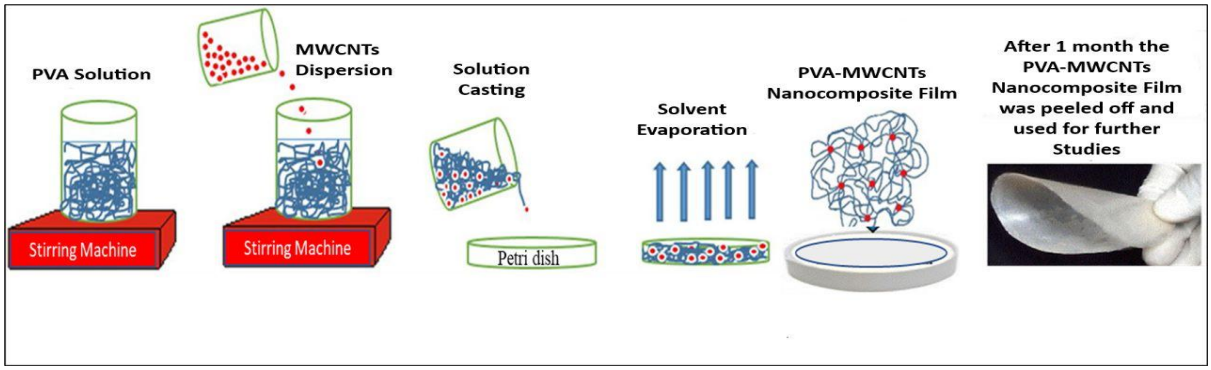

Fig.1. Solution Casting method of PVA-MWCNT Nanocomposites

Characterizations:

The crystal structure and morphology of the films were investigated with an X-ray diffractometer (SHIMADZU XRD-7000) in the scattering range 2θ of 10° to 80°. The interplanar distance between the planes (d) is determined by applying Bragg's formula ($2d\sin\theta = n\lambda$), where θ, n and λ are the Bragg angle, spectral order, and wavelength (0.15406 nm) of the target material (CuK_α), respectively. The FEI Quanta-250 SEM coupled device with energy dispersive X-ray detectors 10kV is used for the surface morphological studies.

AUV-Vis's spectrophotometer (SHIMADZU UV-1800 series) in the 190–1100 nm range was used to acquire the absorption data for all UV–Visible absorption and transmittance studies. The presence of multi-walled carbon nanotubes in the crosslinked nanocomposites was investigated using FTIR spectroscopy. The FTIR spectrometer (SHIMADZU FTIR 8400S) was used to obtain the FTIR spectra in the 400–4000 cm^{-1} range. The Raman spectra of the prepared nanocomposite films were obtained by using a Laser Micro Raman Spectrometer (LAB RAM HR Evolution) in the 200-1500 cm^{-1} range. The INDOSAW-SK068 system with variation of temperature measured the electrical conductivity of the samples.

III. Results and Discussion

XRD Analysis:

The typical X-ray diffraction patterns for pure PVA and PVA/MWCNT composite films with 0.3, 0.6 and 0.9 wt. Concentrations are shown in Fig. 2. The XRD pattern of pure PVA exhibited a large specific diffraction peak observed at a scattering angle ($19°<2\theta<20°$) representing the "d" spacing value of 0.45 nm, which is a typical result for high molecular-weight amorphous polymer. The patterns show a small and sharp peak displayed at $2\theta=37.5°$and $2\theta=63.30°$ for composite films, corresponding to peak diffraction associated with MWCNTs.

The pure PVA and composite films showed another broad and low-intensity crystalline peak at a 2θ position around ~ 43.2°. After nanotubes were dispersed into the PVA matrix, the XRD patterns of nanocomposites only showed the PVA diffraction peaks. This demonstrates that nanotubes were uniformly dispersed in the PVA matrix. There are no changes found in the PVA matrix structure after MWCNTs are dispersed, owing to the abundance of hydroxyl groups that can be present in its backbone. This shows the homogeneity and successful synthesis of composite films incorporating with MWCNTs. It can be seen from Fig.2 that the broad peak of the PVA polymer becomes more broadened with increasing nanotube concentration.

This is evidence of the increase of the amorphous phase in composite films in comparison with the pure PVA film.

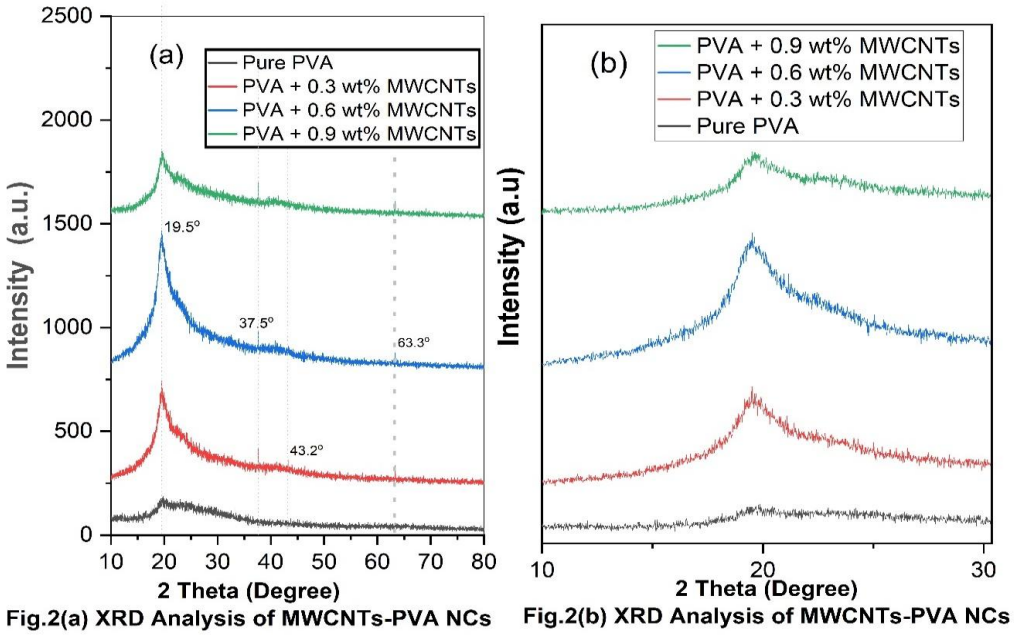

Fig.2 XRD Pattern of MWCNT incorporated PVA nanocomposites.

Surface Morphology:

The surface morphology of PVA nanocomposite films after being reinforced with MWCNT was observed using SEM. Fig.3 shows the images of 0.6wt.% PVA/MWCNTs composite films. The films' morphologies are similar, and it is observed that the roughness of the films increased with MWCNT concentration. The smooth surface morphology of the pure PVA film is observed. Therefore, the semi-crystallinity of PVA is expected to be sub-microscopic. MWCNTs are uniformly distributed throughout the PVA matrix, as observed in SEM micrographs. Compared to pure polymer, this determines the flexibility and strength of composites. The presence and dispersion of 0.3 and 0.9 wt.%, MWCNTs in the PVA matrix are also observed. The film had no cracks but many small black patches on the upper surface. On the top surface of the film, the surface morphology of the composite film displayed aggregates or particle fragmentation. With increasing MWCNTs content in the composite films, the size of particle clusters also increased. On the other hand, the compatibility of MWCNTs and PVA polymer matrices stays isotropic and homogeneous.

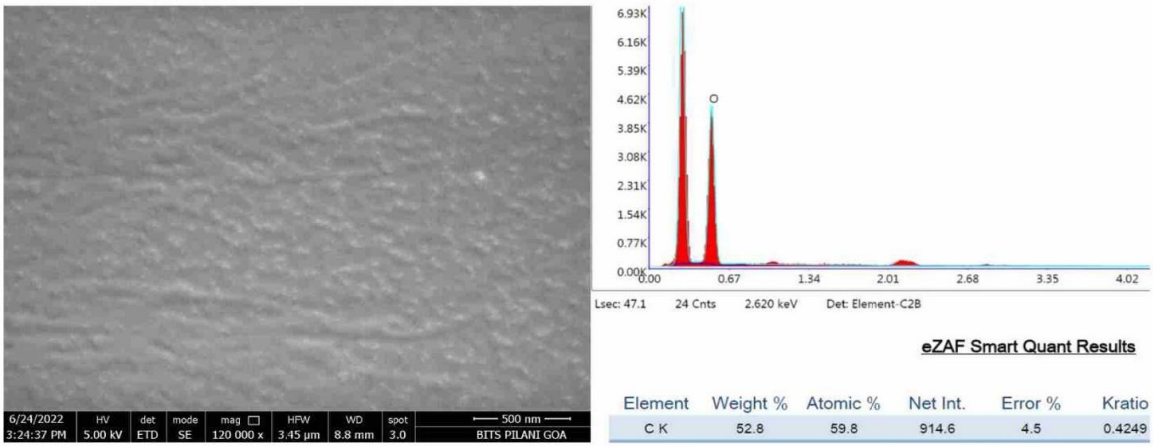

Fig.3 Morphology and Elemental Analysis of MWCNT incorporated PVA nanocomposites.

UV-Vis Spectroscopy:

An optical absorption spectrum is a method for determining optical band constants, analyzing complex compositions, and understanding pure and composite polymers' band structure and electrical properties. The pure PVA film had limited absorption in the visible light range. In contrast, the composite films have high absorption from the visible to UV light range, as shown in Fig.4. Furthermore, at a lower wavelength, the absorption of composite films increases significantly. It can be shown that their UV absorption properties are fully enhanced after nanotubes disperse uniformly in PVA polymer [8]. As a result, the composite films have fine ultraviolet glossy shield characteristics, but their transparency in the visible light region (from 400-800 nm) is not satisfactory. These results have shown that the nanocomposite films absorbed a wide range of radiation.

The absorption edge of the composite films shifts to longer wavelengths with an increase in the concentration of MWCNTs, confirming the amorphous nature of PVA and the creation of new hydrogen bonds in the composites. The shift in wavelength is mainly due to the hydrogen bonding between the nanotubes and -OH groups of PVA. Few absorption peaks were observed at 295nm and 306nm in the spectra of composite films consisting of 0.6 wt.% and at 407-430nm in those consisting of 0.9 wt.%. The n-π* transition and π-π* transitions are responsible for these absorption bands [9]. The observed changes in energy levels symbolize the polymers containing unsaturated bonds, such as C=O or C=Cand are most prominent in the terminal head of the polymer matrix.

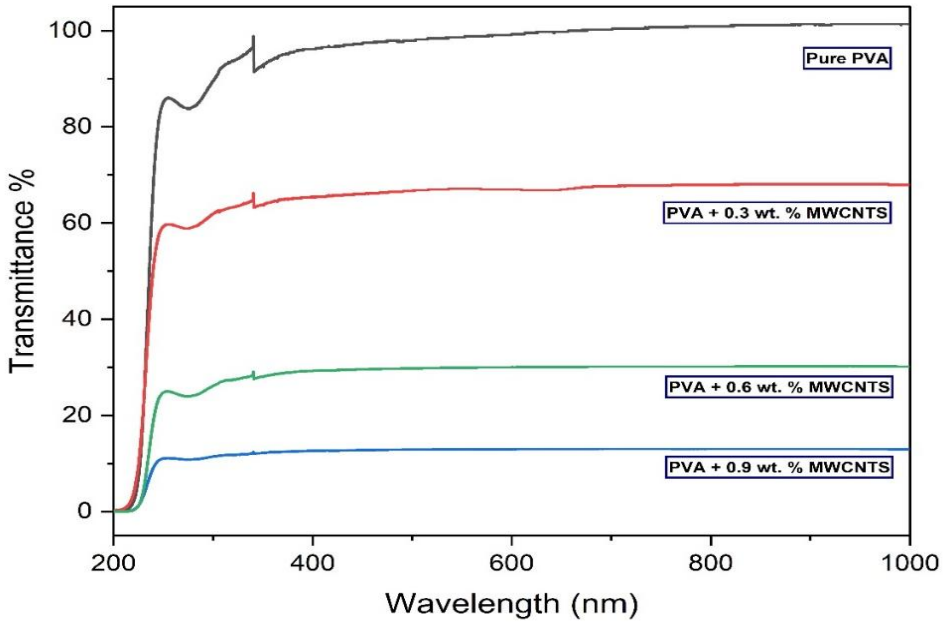

Fig. 4 Transmittance of PVA-MWCNT nanocomposite films.

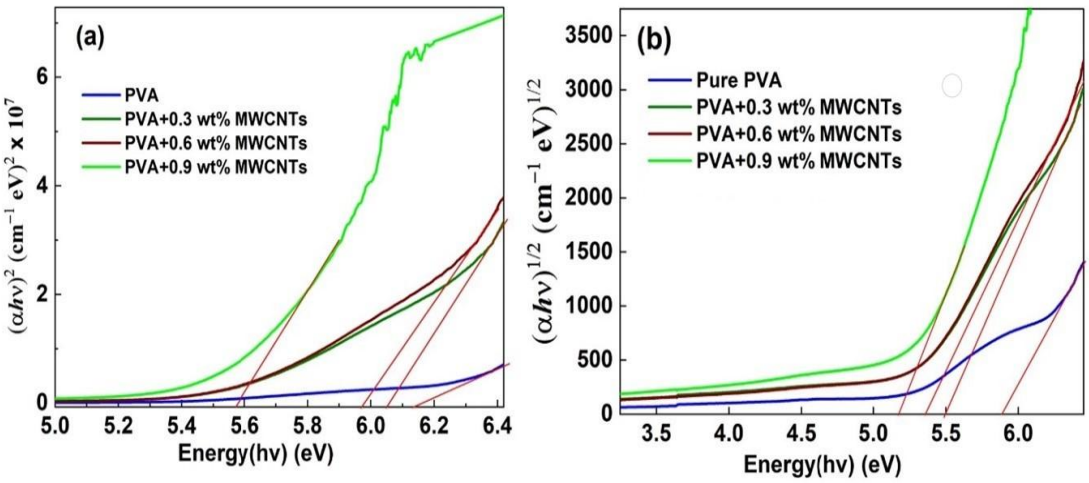

Fig.5. (a) Direct (b) Indirect bandgap energies of PVA-MWCNT nanocomposite films

Fourier Infrared Transform Spectroscopy (FTIR) studies:

The investigation of polymer composite structures can be done using FTIR Spectroscopy. It gives the occurrence of interaction between the various molecular functional groups according to the induced charges in the vibration modes and band positions. Fig.6 shows FTIR spectra of MWCNT-PVA nanocomposite films with different weightage percentages. The broader band near 3446 cm^{-1} shows the presence of the OH group. The peak at 2920 cm^{-1} is due to the presence of CH_2. The peak at 2852 cm^{-1} gives the presence of CH. The band in the range 1724–1670 cm^{-1} is attributed to C = O vibration from acetate groups due to hydrolysis.

The FTIR spectra of the MWCNT with PVA composite and neat PVA were similar. However, a slight shift was detected. The shift of absorption bands at 1629 cm^{-1} and 1436 cm^{-1} of -COO asymmetric and -COO symmetric vibrations, respectively, was also observed in the spectrum of the coated nanoparticles, suggesting the absorption of PVA on the nanoparticles.

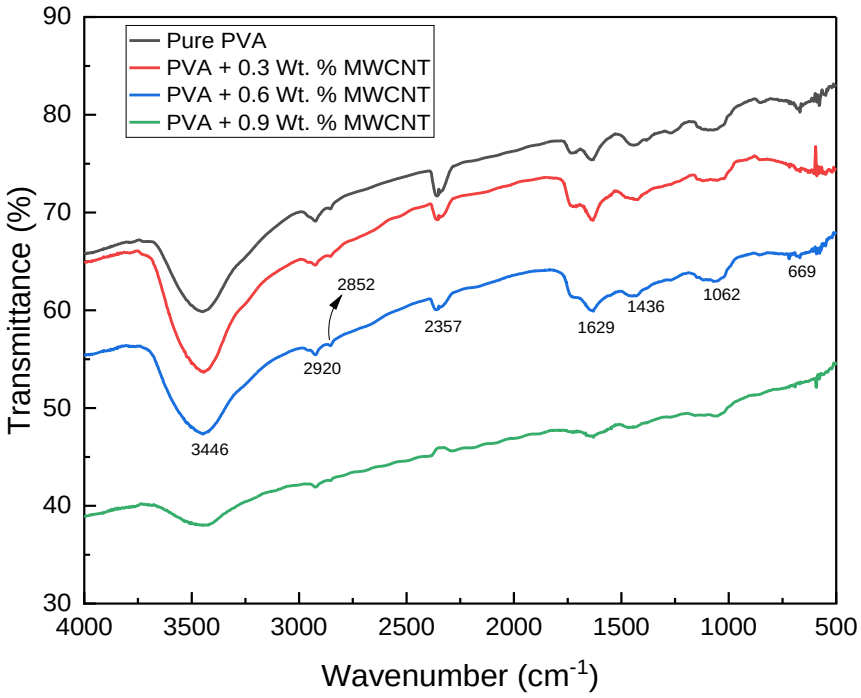

Fig.6. The FTIR spectra of the PVA-MWCNT nanocomposite films.

Raman Spectra Studies:

Raman analysis enables the characterization of carbon-based materials by showing characteristic spectra of sp^3, sp^2, and sp carbons, including disordered carbons, fullerene, and CNT (9). Raman spectra of PVA-MWCNT composites, measured at 532 nm laser excitation, showed two major bands in the spectra, the G band (graphite band) and the D band. Both bands are observed at around 1349 and 1442cm ^{1}, respectively (Fig. 7). The G band denotes the ordered high-frequency in-plane stretching of C-C bonds, while the D band is a disorder or defect present in the CNT sample [10]. The results overall are in accordance with theoretical expectations [11].

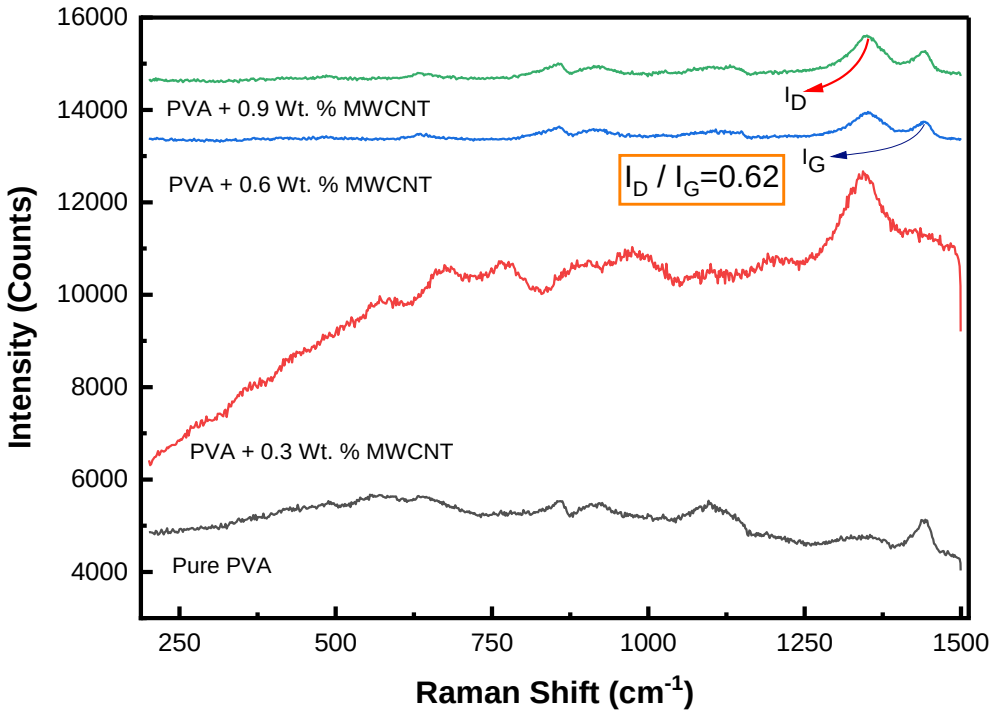

Fig.7. The Raman Spectra of PVA-MWCNT nanocomposite films

Electrical DC Conductivity:

Using a probe station and a thermal chuck with an electronic temperature controller, the electrical conductivity of the composite films was measured as a function of the sample temperature. The DC conductivity of each sample is determined by measuring its resistance through a piece of the material and utilizing the sample size to estimate the following equation [12].

$\sigma = (t/RA)\ S/cm^{1}$

Where t (cm) is the sample thickness, A (cm^2) is its area, and R (ohm) is the resistance of the material. Fig. 8 shows the DC conductivity varies with temperature in MWCNTs incorporated Poly Vinyl Alcohol (PVA) nanocomposite films as a function of dopant amount by weight percent. Proton carrier concentration has been increased, which is principally responsible for the rise in ionic conductivity with dopant composition. The enormous. The amplitude of the polymer segmental motion helps the protons flow more through the polymer matrix. Amorphous regions have substantially higher segmental mobility of polymer chains than crystalline regions.

The increase in electrical conductivity and decrease in activation energies after incorporation of CNTs may be due to the change in amorphous structure (improvement of cross-links and grain size) and decrease in grain boundary domains [13].

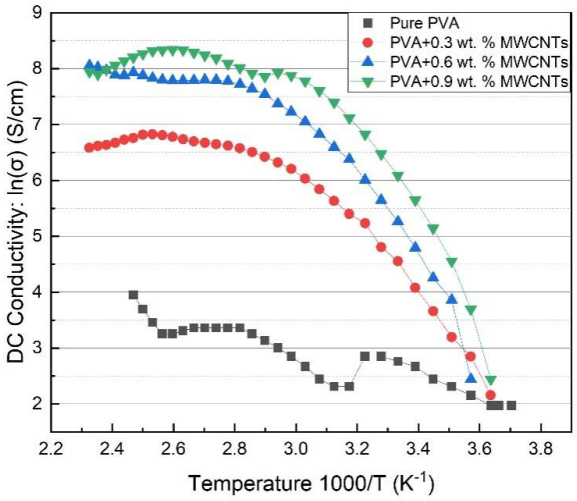

Fig.8. DC Electrical conductivity of PVA - MWCNTs Nanocomposites.

IV. Conclusion

MWCNT-incorporated PVA nanocomposite films were prepared by using the solution casting method. Structure, Surface morphology, FTIR spectra, Raman spectra, optical transmission, and electrical conductivity of PVA/MWCNT nanocomposite with and without MWCNT incorporation manufactured by simple casting method were analyzed. As the content of MWCNT increases, it is observed that the roughness of the films increases. The MWCNT agglomeration is also being increased with the content of incorporation MWCNTs. By using FTIR and Raman spectra, we confirmed the proper incorporation of MWCNT into PVA films. It is also observed that both the direct and indirect bandgaps decrease with an increase in CNT content. The electrical conductivity increased with increasing MWCNT content.

Acknowledgements

The authors are thankful to the Head, Dept. of Physics, UCE(A), Osmania University, Hyderabad, Telangana, for allowing us to use the experimental facilities available at the Department of Physics.

References

[1]. Camargo PHC, Satyanarayana KG, Wypych F. Nanocomposites: synthesis, structure, properties and new application opportunities. Mater Res. 2009 Mar;12:1–39.
[2]. Maghfirah A, Yudianti R, Fauzi, Sinuhaji P, Hutabarat LG. Preparation Of Poly(Vinyl) Alcohol – Multiwalled Carbon Nanotubes Nanocomposite As Conductive And Transparent Film Using Casting Method. J Phys Conf Ser. 2018 Dec;1116(3):032017.
[3]. Paine DC, Yeom HY, Yaglioglu B. Transparent Conducting Oxide Materials and Technology. In: Flexible Flat Panel Displays [Internet]. John Wiley & Sons, Ltd; 2005 [cited 2022 Dec 11]. p. 79–98. Available from: https://onlinelibrary.wiley.com/doi/abs/10.1002/0470870508.ch5
[4]. Iijima S. Helical microtubules of graphitic carbon. Nature. 1991 Nov;354(6348):56–8.
[5]. Hu L, Hecht DS, Grüner G. Percolation in Transparent and Conducting Carbon Nanotube Networks. Nano Lett. 2004 Dec 1;4(12):2513–7.
[6]. Wagner HD, Lourie O, Feldman Y, Tenne R. Stress-induced fragmentation of multiwall carbon nanotubes in a polymer matrix. Appl Phys Lett. 1998 Jan 12;72(2):188–90.
[7]. Hu L, Hecht DS, Grüner G. Infrared transparent carbon nanotube thin films. Appl Phys Lett. 2009 Feb 23;94(8):081103.
[8]. Sahoo BP, Tripathy DK. Polymer Nanocomposites for Electronics, Dielectrics, and Microwave Applications. In: Tripathy DK, Sahoo BP, editors. Properties and Applications of Polymer Nanocomposites: Clay and Carbon Based Polymer Nanocomposites [Internet]. Berlin, Heidelberg: Springer; 2017 [cited 2022 Dec 15]. p. 25–36. Available from: https://doi.org/10.1007/978-3-662-53517-2_2
[9]. Kumar P, Khan N, Kumar D. POLYVINYL BUTYRAL (PVB), VERSETILE TEMPLATE FOR DESIGNING NANOCOMPOSITE/COMPOSITE MATERIALS:A REVIEW [Internet]. 2016 [cited 2022 Dec 15]. Available from: https://www.semanticscholar.org/paper/POLYVINYL-BUTYRAL-(PVB)%2C-VERSETILE-TEMPLATE-FOR-Kumar-Khan/3f65efad16b1825ebcbab99aeca0a38d26f33582
[10]. Malikov EY, Muradov MB, Akperov OH, Eyvazova GM, Puskás R, Madarász D, et al. Synthesis and characterization of polyvinyl alcohol based multiwalled carbon nanotube nanocomposites. Phys E Low-DimensSyst Nanostructures. 2014 Jul 1;61:129–34.
[11]. Zawawi NA, Majid ZA, Rashid NAA. Adsorption and desorption of curcumin by poly(vinyl) alcohol-multiwalled carbon nanotubes (PVA-MWCNT). Colloid Polym Sci. 2017 Oct 1;295(10):1925–36.
[12]. Kumar NBR, Crasta V, Praveen BM. Dielectric and electric conductivity studies of PVA (Mowiol 10-98) doped with MWCNTs and WO3 nanocomposites films. Mater Res Express. 2016 May;3(5):055012.
[13]. Trawiński B, Bochentyn B, Gostkowska N, Łapiński M, Miruszewski T, Kusz B. Structure and thermoelectric properties of bismuth telluride—Carbon composites. Mater Res Bull. 2018 Mar 1;99:10–7.